ОБЪЕДИНЕННЫЙ
ИНСТИТУТ
ЯДЕРНЫХ
ИССЛЕДОВАНИЙ

Дубна

E1 - 5256

Z.S. Strugalski, I.V. Chuvilo, T. Gemesy,
I.A. Ivanovskaya, Z. Jabłoński, T. Kanarek,
S. Krasnovsky, L.S. Okhrimenko, G. Pinter

NEUTRAL DECAY MODES OF THE η^0 PARTICLE

ЛАБОРАТОРИЯ ВЫСОКИХ ЭНЕРГИЙ

1970

E1 - 5256

Z.S. Strugalski, I.V. Chuvilo, T. Gemesy,
I.A. Ivanovskaya, Z. Jabłoński, T. Kanarek,
S. Krasnovsky, L.S. Okhrimenko, G. Pinter

NEUTRAL DECAY MODES OF THE η^0 PARTICLE

Submitted to Nucl. Phys.

1. Introduction

In recent years, starting from 1962, many experimental works have been devoted to a study of η^0 meson decays[1-17]. As is well known, there are great inconsistencies among the various experiments which report etas decaying into neutrals. In many experiments[2,4,5,8,9,13] the indirect methods for determination of the branching ratios of η^0 neutral decay channels ($\eta^0 \to 2\gamma^0$, $\eta^0 \to \pi^0\gamma\gamma$, $\eta^0 \to 3\pi^0$) have been used, i.e. in any single event under investigation not all gamma-quanta have been observed because of very small registration efficiency. The direct methods, in which the possibility exists to observe all gamma-quanta emitted, and to measure their energies and angles of emission, are connected with the heavy liquid bubble chamber techniques[10,14,15,17]. The investigations performed in these chambers concern with very small statistics, however. It should be pointed out, that in our work the simultaneous investigations of all neutral decay modes of η^0 meson have been performed [15], in contrast to other works in which some definite neutral decay modes have been investigated only.

In this article our final results of η^0 decay modes investigations are presented.

2. Method

The η^0 neutral decay modes have been studied by means of the Joint Institute for Nuclear Research 550 x 280 x 160 mm^3 xenon bubble chamber irradiated with a 2.34 GeV/c π^+ beam. The scanning of photographs was done for the interactions of $\pi^+ - Xe$, occuring in 290 x 120 x 50 mm^3 central fiducial volume, with one secondary observable charged particle stopping in the chamber and accompanied by any number of gamma-quanta. The selected events can be interpreted as interactions of the type

$$\pi^+ + n \to \underset{\hookrightarrow k\gamma}{X} + p, \quad (k = 0, 1, \ldots), \tag{1}$$

i.e. π^+ with quasi-free neutrons in xenon nuclei /18/. In each event the angles of gamma-quanta emission were estimated with the accuracy $\Delta\Theta_\gamma = (0.5 - 2)^\circ$, and the energies of gamma-quanta - with the accuracy $\Delta E_\gamma / E_\gamma = (15 - 35)$ % /19/.

The gamma-quantum recording probability was estimated for every gamma-quantum taking into account the possibility of measuring its energy with the accuracy better than 35%. The recording probability of gamma-quantum in selected events makes up, in average, 0.82 - 0.86 depending on gamma-quanta number in event. The average recording probability for 2 gamma-quanta events makes up 0.71, for 4 gamma-quanta events - 0.47, for 6 gamma-quanta events - 0.42. The average gamma-quantum observation probability equals 94%.

3. Experimental Results

This experiment uses over 500 000 stereophotographs of the chamber. The following numbers of events have been found: 2 gamma events - 746, 4 gamma events - 306, 6 gamma events - 51.

a). Two gamma-quanta events

In fig. 1 the distribution of γ-γ effective mass $M_{2\gamma}$ is presented taking into account the statistical weight of each event. The shaded part of the histogram represents the background from such three[x] and four gamma-quanta events, in which only two gammas are converted within the chamber volume. The background was estimated from the $\gamma-\gamma$ combinations in the samples of three and four gamma-quanta events ($M^{2\gamma}_{3\gamma}$ and $M^{2\gamma}_{4\gamma}$). The contamination of wrong events was estimated from the numbers of events registered with three and four gamma-quanta. The background from the five and six gamma-quanta events is small, being less than 1 event.

Two groups of events are observed in the distribution presented in fig.1: the first at the π^0 meson mass value, 804 ± 35 events, and the second one at the η^0 meson mass value, 195 ± 20 events.

b) Four gamma-quanta events

In the sample of four gamma-quanta events the effective masses $M^{2\gamma}_{4\gamma}$ of $\gamma-\gamma$ combinations were estimated, and the all events were divided into three groups: 1. $\pi^0-\pi^0$ events, 2. $\pi^0\,\gamma\gamma$ events, 3. $\pi^0-\eta^0$ events. Two gamma-quanta combinations are assumed to be π^0 meson if the value of $M^{2\gamma}_{4\gamma}$ was lying into 90-180 MeV interval, and to be η^0 meson for $M^{2\gamma}_{4\gamma}$ value being in 400-700 MeV interval.

---

[x] Assuming the three gamma-quanta events to be the "true" three gamma events, i.e. $\omega^0 \to \pi^0\gamma \to 3\gamma$, for example.

In fig.2 the effective mass distribution of 100 $\pi^0\gamma\gamma$ events selected is shown. The recording probability of the events is taken into account. The solid curve represents the distribution of random $\pi^0\gamma\gamma$ combinations estimated by means of the special Monte-Carlo programme and normalized to the number of events with mass values $M_{4\gamma}(\pi^0\gamma\gamma) < 400$ MeV. For evaluation of this curve the angular and energy spectra of gamma-quanta from the $\pi^0\gamma\gamma$ sample of selected events were used. The peak is observed above the background level at mass value interval 500-600 MeV. It can be explained as the indication for existence of η^0 meson decays according to the $\pi^0\gamma\gamma$ channel. The total number of such η^0 events estimated equals 40 $\pm$ 10.

The other way of the $\eta^0 \to \pi^0\gamma\gamma$ decay mode selection has been used as well. In fig. 3 the distribution of effective mass of γ-γ combinations from the $\pi^0\gamma\gamma$ and $\pi^0\eta^0$ events is presented for the pairs of gamma-quanta which combinations do not form the π^0-meson mass values. The shaded parts of histogram represent the non-simple events, i,e. such events in which the two γ-γ combinations (from the six possible for four gamma-quanta events) give the effctive mass values correponding to the π^0 meson mass. From such events the two values of γ-γ combinations were included in the histogram if the first of the mass values was less than 300 MeV and the second one higher than 300 MeV. The solid curves represent the distributions of gamma-quanta combinations for π^0 and η^0 mesons from fig.1. The normalization was performed for the total number of events with mass values $M_{\gamma\gamma} < 300$ MeV and $M_{\gamma\gamma} > 400$ MeV. One can see from fig.3 that the main part of the $\pi^0\gamma\gamma$ events is coming from the $\pi^0\eta^0$ and $\pi^0\pi^0$ events in which the value of effective mass of one of π^0's do not hit within the

90-180 MeV interval. The number of such π^0-π^0 events is in good agreement with the expected one at the 30% π^0 meson effective mass determination accuracy. In fig.3 some number of events with the 300-400 MeV mass value interval is also seen. In the work of S. Shapiro /16/ the invariant mass spectrum of the two gamma-quanta from $\eta^0 \to \pi^0 \gamma\gamma$ decay has been evaluated assuming the matrix element squared for this decay is $M^4_{\gamma\gamma}$ (fig.4/16/). Comparison of this spectrum with the one from fig. 3 allows to suppose the group of events lying within 300-400 MeV mass values interval to be the events of the $\eta^0 \to \pi^0 \gamma\gamma$ decays. This supposition seems to be true also from the analysis of 4 gamma-quanta effective mass distribution of events considered. From fig.5 one can see the 27 well identified events lying near the η^0 mass value. The other 20 events lying near the η^0 mass value (shaded part of the histogram) are such events which can be not well identified. So, the evaluation of the number of $\eta^0 \to \pi^0 \gamma\gamma$ decays (27-47 events) agrees well with this performed before (40$\pm$ 10 events).

In fig.6 the energy spectrum of the gamma-quanta from the $\eta^0 \to \pi^0 \gamma\gamma$ events in the center of mass system of the η^0 meson is given. The dotted line presents the theoretical evaluated spectrum from the work of C. Baltay et al./13/. Good agreement between the experimental and theoretical spectra is observed.

c) Six gamma-quanta events

In fig.7 the six gamma-quanta combination effective mass spectrum for six gamma-quanta events is shown. The statistical weights of events are taken into account in the distribution presented. The sample of six gamma-quanta events considered contain the events being the $\eta^0 \to 3\pi^0$ decays and the events being the non-resonance production of $3\pi^0$ mesons. The curve 1 in fig.7 represents the

η^0 meson effective mass distribution taking into account the mass estimation errors and the curve 2 is the phase space for non-resonant $3\pi^0$'s production. For evaluation of the curve 2 the Monte-Carlo programme has been used/20/. It follows from comparison of the phase space curve with the experimental data that the number of non-resonant $3\pi^0$ events at mass values region less than 550 MeV can be practically neglected. The curve 1 has been normalized to the total number of $3\pi^0$ events at mass values region $M_{6\gamma} < 550$ MeV, therefore. The distribution of the non-resonant $3\pi^0$ events, after substraction of the number of the $\eta^0 \to 3\pi^0$ mesons, is presented in fig.8. The phase space is drawn in this fig.8, too. Thus, separating the $\eta^0 \to 3\pi^0$ events and the $3\pi^0$'s non-resonant events we have estimated: 73 events of $\eta^0 \to 3\pi^0$ decays and 41 events of non-resonant $3\pi^0$'s generation.

In addition to the events considered above 50 events exist in which the number of gamma-quanta, 5 or 6, cannot be determined because of very strong shower interlacing. Those events have been separated into two parts of 5 and 6 gamma-quanta events in proportion 83-47. This relation follows from the good resolved numbers of five and six gamma-quanta events recorded in our experiment. The number of six gamma-quanta events evaluated has been divided, in one's turn, into two parts of non-resonant $3\pi^0$ events and of the $\eta^0 \to 3\pi^0$ events in the proportion 41:73. Taking into account the registration probability the numbers of events were estimated: 36 events of $\eta^0 \to 3\pi^0$ and 20 events of $3\pi^0$'s from non-resonant reactions. In that way the number of $\eta^0 \to 3\pi^0$ events estimated is equal to 109 ± 30.

Supposing some other neutral decay modes do not exist, we estimate the following relations:

$$\frac{N(\eta^0 \to 2\gamma)}{N(\eta^0 \to \text{all neutrals})} = (57 \pm 9)\%,$$

$$\frac{N(\eta^0 \to \pi^0 \gamma\gamma)}{N(\eta^0 \to \text{all neutrals})} = (11 \pm 3)\%, \qquad (2)$$

$$\frac{N(\eta^0 \to 3\pi^0)}{N(\eta^0 \to \text{all neutrals})} = (32 \pm 9)\%.$$

4. Discussion

In spite of big statistical errors, we are thinking a serious indication exists for evidence of the appreciable amount of the $\eta^0 \to \pi^0 \gamma\gamma$ decay mode. Our last result does not disagree with the results of recent works/9,10,13/ which are interpreted as the evidence of absence of the $\eta^0 \to \pi^0 \gamma\gamma$ decay mode, however. In those works as the upper limit for the ratio $(\eta^0 \to \pi^0\gamma\gamma)/(\text{all neutr.})$ the values (12–17)% have been done.

It should be noted the latest result $(\eta^0 \to \pi^0\gamma\gamma)/(\text{all neutr.}) = (12.2 {}^{+5.2}_{-4.4})\%$ agrees well with the our one/21/.

Reference s

1. M. Chrétien, F. Bulos, H.R. Crouch, Jr. R.E. Lanou, J.T. Massimo, A.M. Shapiro, J.A. Averell, C.A. Bordner, A.E. Brenner, D.R. Firth, M.E. Low, E.E. Ronat, K. Strauch, J.C. Street, J.J. Szymanski, A. Weinberg, B. Nelson, I.A. Pless, L. Rosenson , G.A. Salandin, R.K. Yamamoto, L. Guerriero, F. Waldner. Phys.Rev.Lett., 9, 127 (1962).

2. F.S. Crawford, L.J. Lloyd, E.C. Fowler. Phys.Rev.Lett., 10, 546 (1963).

3. C. Bacci, G. Penso, G. Salvini, A. Wattenberg, C. Mencuccini, R. Querzoli, V. Silvestrini. Phys.Rev.Lett., 11, 37 (1963).

4. M. Foster, M. Peters, R. Hartung, R. Matsen, D. Reeder, M. Good, M. Meer, F. Loeffler, R. Mc Ilwain. Phys.Rev., 138B, 652 (1965).

5. G. Di Guigno, R. Querzoli, G. Troise, F..Vanoli, M. Giorgi, P. Shiavon, V. Silvestrini. Phys.Rev.Lett., 16, 767 (1966).

6. M.A. Wahlig, E. Shibata, I. Manneli. Phys.Rev.Lett., 17, 221 (1966).

7. J. Grunhaus. Thesis . Columbia University, 1966/Nevis 156/.

8. M. Feldman, W. Frati, R. Gleeson, J. Halpern, M. Nussbaum, S. Richert. Phys.Rev.Lett., 18, 868 (1967).

9. S. Buniatov, E. Zavatini, N. Deinet, H. Muller, D. Schmitt, H. Staudenmaier. Phys.Lett., 25B, 560 (1967).

10. F. Jacquet, U. Nguyen-Khac, C. Baglin, A. Bezaguet, B. Degrange, R.J. Kurz, P. Musset, A. Haatuft, A. Halsteinlid, J.M. Olsen. Phys. Lett., 25B, 574 (1967).

11. P. Bonamy, P. Sonderegger. Heidelberg Conference, 1967.

12. R.J. Cence, Y.Z. Peterson, V.J. Steger, C.B. Chiu, R.D. Eandi, A.C. Helmholz, R.W. Kenney, B.J. Moyer, J.A. Poirier, W.B. Richards. Phys.Rev.Lett., 19, 1393 (1967).

13. C. Baltay, P. Franzini, J. Kim, R. Newman, N. Yeh , L. Kirsch. Phys.Rev.Lett., 19, 1495 (1967).

14. F.W. Bullock, M.J. Estch, E. Fleming-Tompa, M. Govan, C. Henderson, A.A. Owen, F.R. Stannard. Phys.Lett., 27B, 402 (1968).

15. Z.S. Strugalski, I.V. Chuvilo, I.A. Ivanovskaya, L.S. Okhrimenko, B. Niczyporuk, T. Kanarek, Z. Jablonski, B. Slowinski. JINR Preprint, E1-3100, Dubna (1967).

16. S. Shapiro. Thesis. Columbia University, 1969 (Nevis 174).

17. B. Degrange. Thesis. Universite de Paris , 1969.

18. Z. Strugalski, T. Siemiarczuk. Phys.Lett., 13, 347 (1964);
M. Daszkiewicz, B. Slowinski, Z. Strugalski. Journ. of Nucl. Phys., (in Russian), 5, 341 (1966).

19. I.A. Ivanovskaya, T. Kanarek, L.S. Okhrimenko, B. Slowinski, Z. Strugalski, I.V. Chuvilo, Z. Jablonski. Instr. and Technik of Exp. (in Russian), 2, 39 (1968).

20. G.I. Kopylov and V.E. Komolova. JINR Preprint, 2027, Dubna (1965).

21. B. Cox, L. Fortuney, J. Golson. Phys.Rev.Lett., 24, 534 (1970).

Received by Publishing Department
on July 20, 1970.

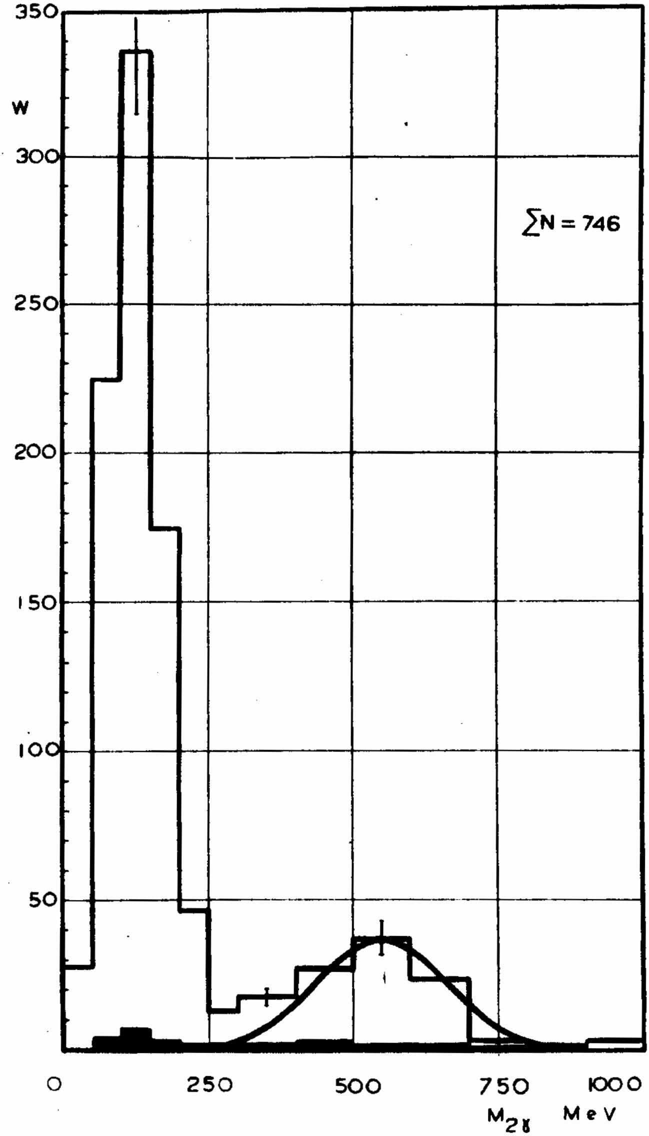

Fig.1. Distribution of $M_{2\gamma}$ in the two gamma-quanta events. The shaded area represents the background from events with number of gamma-quanta more than two. The solid curve shows the Gauss distribution with $\sigma = 120$ MeV.

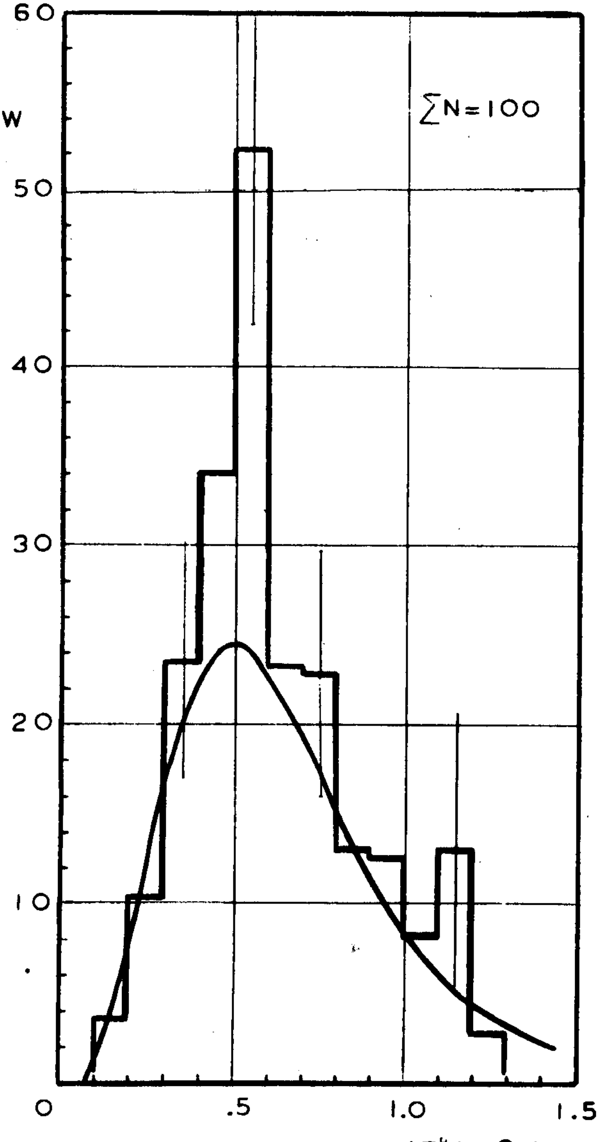

Fig.2. Distribution of $M_{4\gamma}(\pi^0\gamma\gamma)$ in the four gamma-quanta events. The solid curve represents the background estimated by means of Monte-Carlo programme.

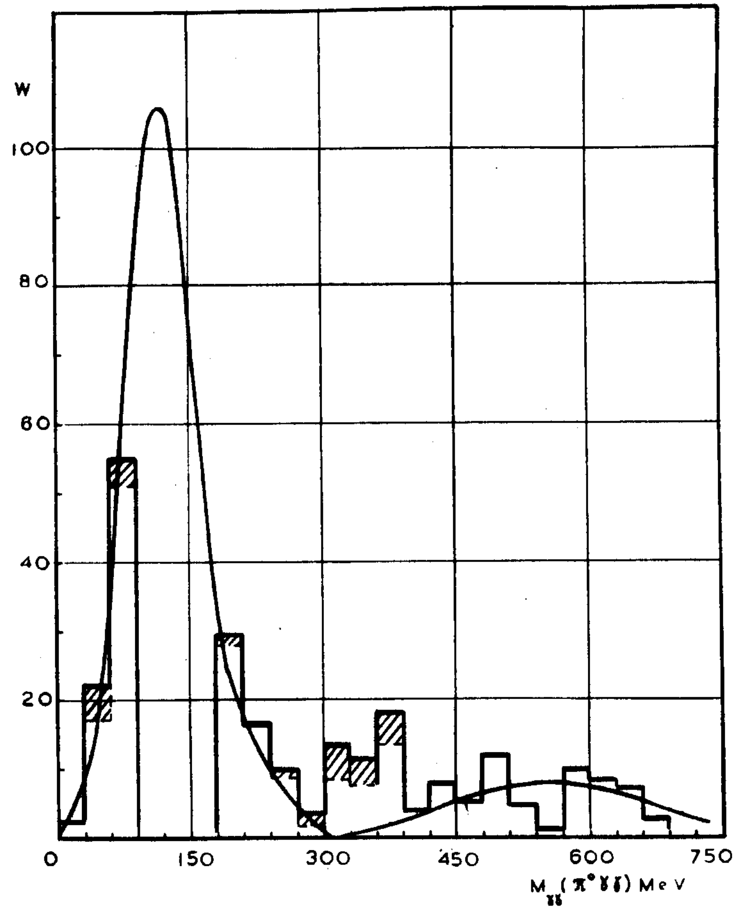

Fig.3. Distribution of $\gamma-\gamma$ combinations from the $\pi^0\gamma\gamma$ and $\pi^0\eta^0$ events for the pairs of gamma-quanta which combinations do not form the π^0 meson mass values. The shaded areas represent the non-simple events. Solid curves - the distributions of effective mass for $\pi^0 \to 2\gamma$ and $\eta^0 \to 2\gamma$ taking into account the errors of mass measurement.

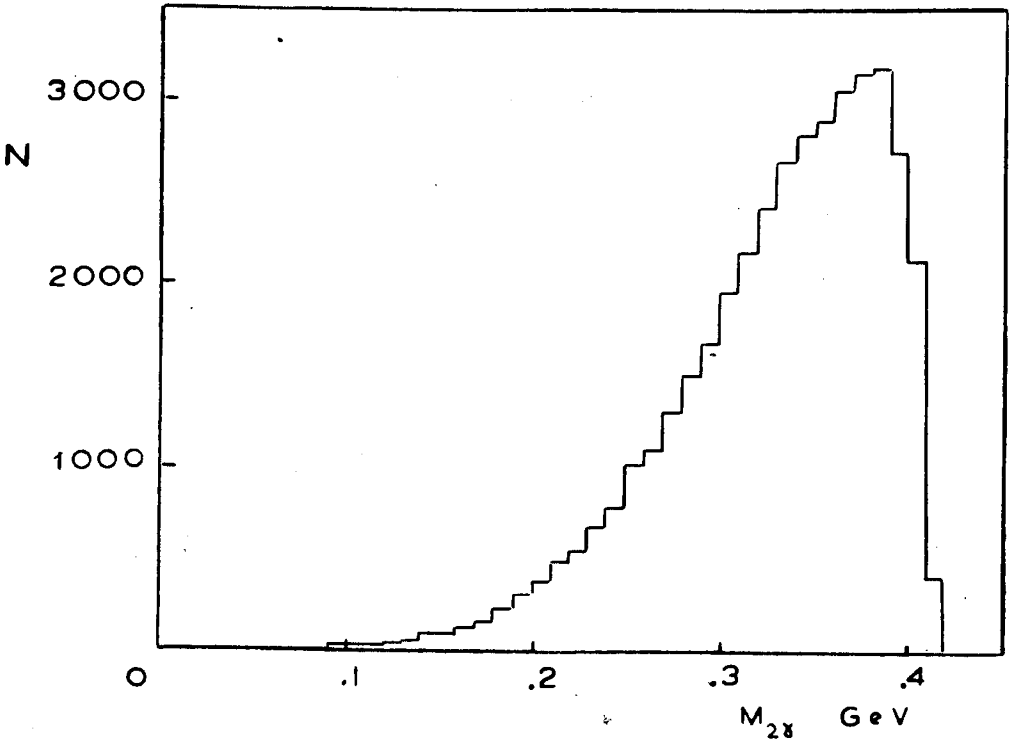

Fig.4. Invariant mass of the two gamma-quanta from $\eta^0 \to \pi^0 \gamma\gamma$ assuming the matrix element squared for the decay is $M_{\gamma\gamma}^4$ /16/.

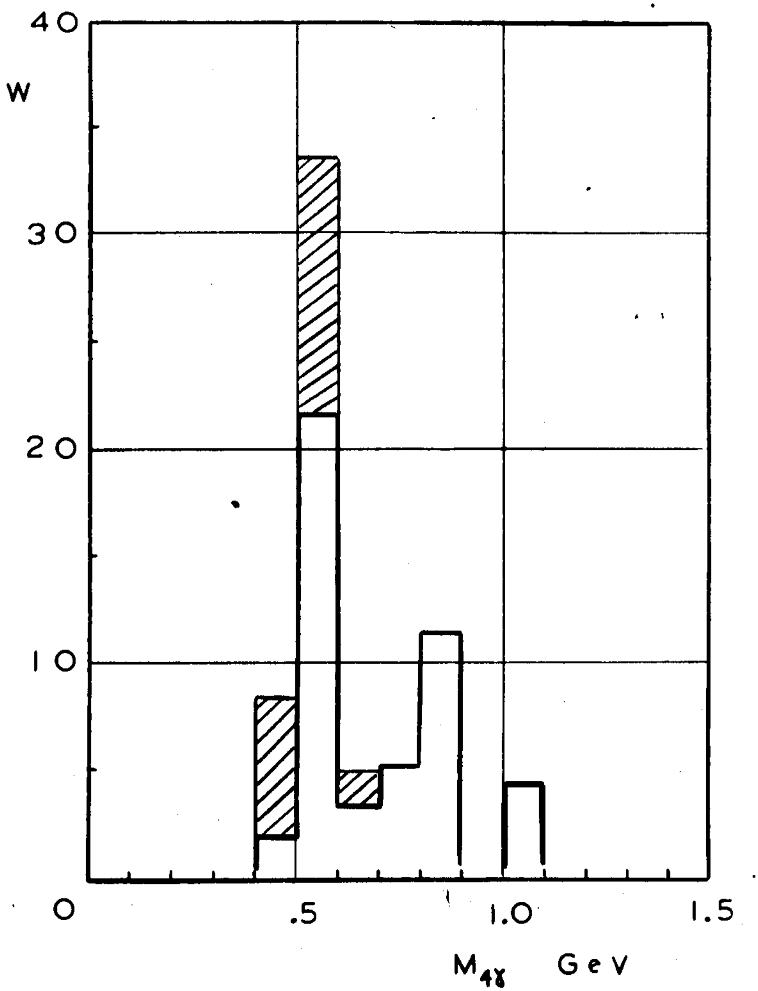

Fig.5. Distribution of four gamma-quanta effective mass for $\pi^0 \gamma\gamma$ events in which the γ-γ effective mass are lying within mass values interval 300 MeV < $M_{\gamma\gamma}$ < 400 MeV. The shaded areas of the histogram represents the non-simple events.

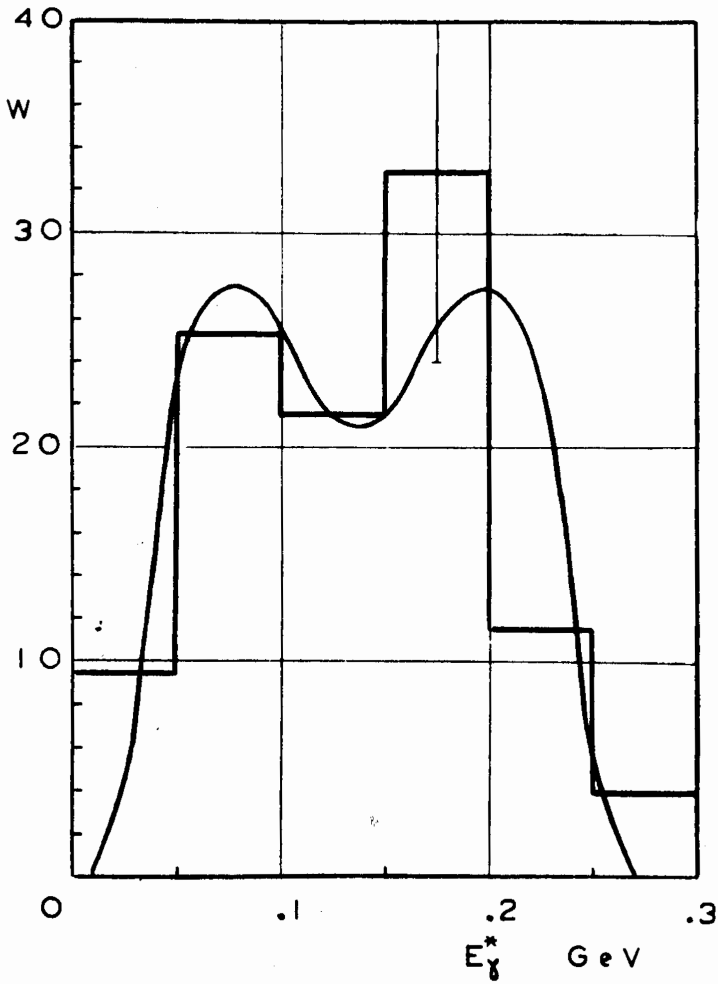

Fig.6. The energy spectrum of the gamma-quanta from the $\eta^0 \to \pi^0 \gamma\gamma$ decay events in the center of mass system of the η^0 meson. The solid curve represents the theoretical spectrum /13/.

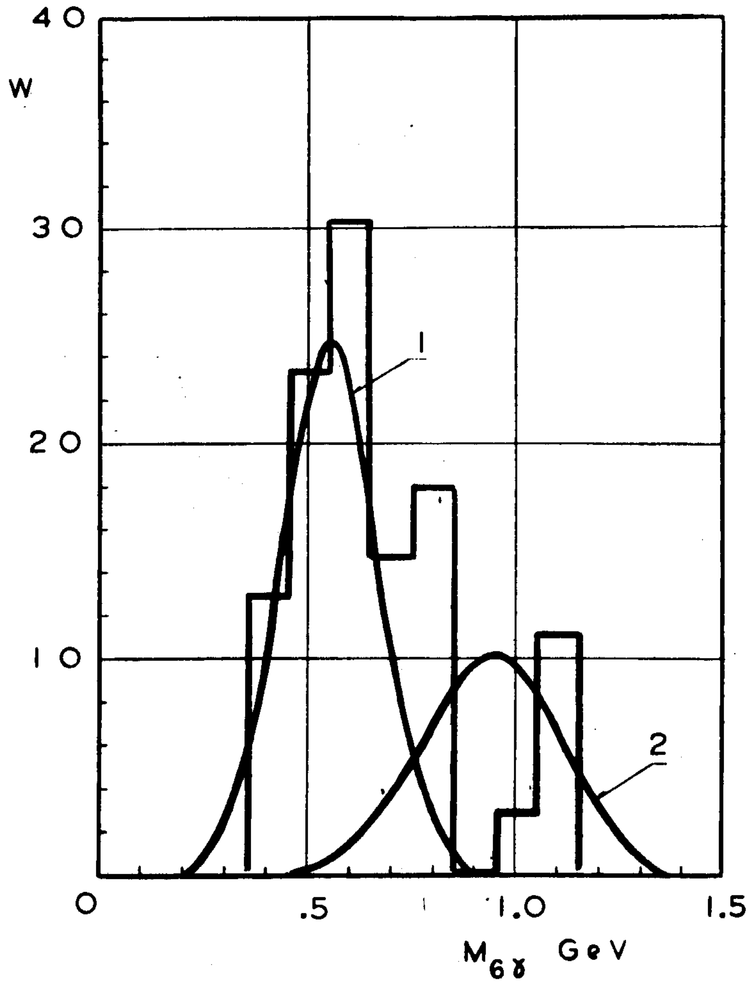

Fig.7. Distribution of the six gamma-quanta effective mass for six gamma-quanta events. The curve 1 - the Gauss distribution for σ = 120 MeV; the curve 2 - the phase space for the reactions $\pi^{+} + n \rightarrow p + 3\pi^{0}$.

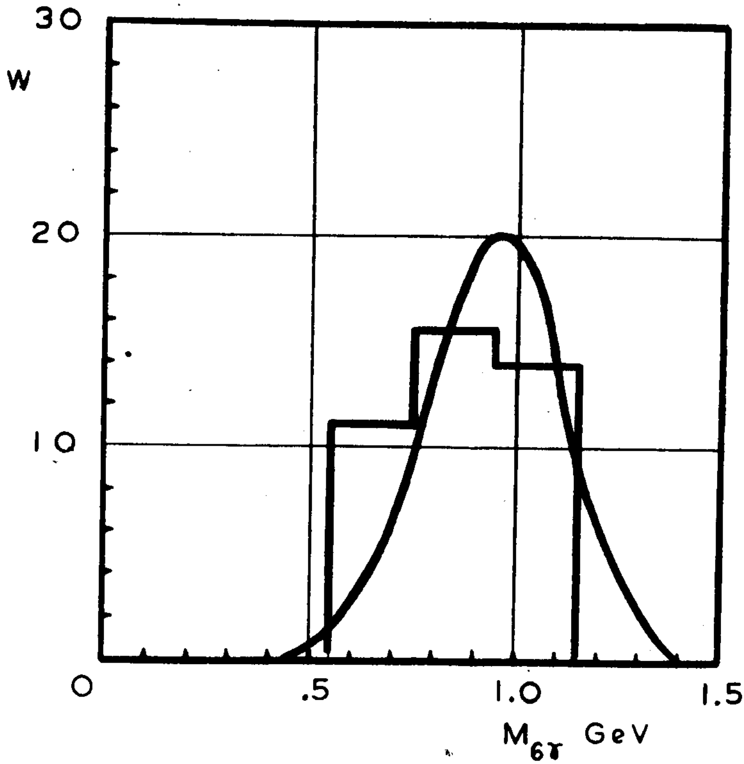

Fig.8. Distribution of effective mass of six gamma-quanta for events being non-resonant production of three π^0 mesons. The solid curve - the phase space for the reaction $\pi^+ + n \rightarrow p + 3\pi^0$.